

Electronic Supplementary Information (ESI)

An INHIBIT logic gate from thiophene derivative using iron and zinc ions as input: Tuning the efficiency on moving from naphthalene to anthracene to pyrene for green luminescent detection of intracellular iron

Arnab Banerjee^a, Animesh Sahana^a, Sudipta Das^a, Sisir Lohar^a, Bidisha Sarkar^b, Subhra Kanti Mukhopadhyay^b, Jesús Sanmartín Matalobos^{c*} and Debasis Das^{a*}

^a*Department of Chemistry, The University of Burdwan, Burdwan, West Bengal, India*

^b*Department of Microbiology, The University of Burdwan, Burdwan – 713104, West Bengal, India,*

^c*Departamento de Química Inorgánica, Facultade de Química, Avda. Das Ciencias s/n, 15782, Santiago de Compostela, Spain.*

Debasis Das <e-mail: ddas100in@yahoo.com>; Tel: +91-342-2533913; Fax: +91-342-2530452

1. Calculation of Quantum Yield

Fluorescence quantum yields (Φ) were estimated by integrating the area under the fluorescence curves using the equation¹,

$$\phi_{\text{sample}} = \phi_{\text{ref}} \times \frac{\text{OD}_{\text{ref}} \times A_{\text{sample}} \times \epsilon_{\text{sample}}^2}{\text{OD}_{\text{sample}} \times A_{\text{ref}} \times \epsilon_{\text{ref}}^2}$$

where A was the area under the fluorescence spectra and OD was optical density of the compound at the excitation wavelength. Anthracene has been used as quantum yield standard (quantum yield is 0.27 in ethanol)² for measuring the quantum yields of PTA and its

Zn²⁺ adduct. For [PTA- Fe³⁺]adduct, tris(2,2'-bipyridyl)ruthenium(II) ($\Phi = 0.042$ in water) has been used.³

2. Calculation of detection limit

To determine the detection limit, fluorescence titration of PTA with Fe³⁺ is carried out by adding aliquots of micro-molar concentration of Fe³⁺. From the concentration at which there was a sharp change in the fluorescence intensity multiplied with the concentration of PTA gave the detection limit.⁴

3. Equations used for calculating detection limit (DL)

$$DL = C_L \times C_T$$

C_L = Conc. of PTA; C_T = Conc. of iron at which fluorescence enhanced.

Thus;

$$DL = 1 \mu M \times 0.01 \mu M = 0.01 \mu M = 1 \times 10^{-8} M$$

4. X-ray crystal structural parameters

Crystal parameters	PTA	ANTA
Molecular formula	C ₂₂ H ₁₅ NS	C ₂₀ H ₁₅ NS
Formula weight	325.41	301.39
Crystal system	Monoclinic	Monoclinic
Space group	P2 ₁ /c	P2 ₁ /c
a/Å	12.6935 (18)	4.3718 (4)
b/Å	9.3300 (12)	13.1396 (12)
c/Å	13.2778 (17)	25.912 (2)

$\alpha/^\circ$	90.0	90.0
$\beta/^\circ$	95.55 (1)	93.433 (5)
$\gamma/^\circ$	90.0	90.0
Z	4	4
$V/\text{\AA}^3$	1565.1 (4)	1485.8 (2)
T/K	100	100
$\lambda/\text{\AA}$	0.7107	0.7107
$\rho/\text{mg m}^{-3}$	1.381	1.347
μ/mm^{-1}	0.21	0.21
Crystal size/mm	$0.68 \times 0.37 \times 0.02$	$0.52 \times 0.11 \times 0.08$
$h/k/l$	$-15 \rightarrow 15/0 \rightarrow 11/0 \rightarrow 16$	$-5 \rightarrow 5/0 \rightarrow 16/0 \rightarrow 32$
$F(000)$	680	632
θ range/°	2.7–24.5°	2.2–26°
T_{\min} and T_{\max}	0.607 and 1.0	0.953 and 1.0
Reflection collected	33038	22444
Independent reflection	3092	3068
R factor (all data)	0.058	0.037
R factor (final)	0.150	0.096

Geometry

All s.u.'s (except the s.u. in the dihedral angle between two l.s. planes) are estimated using the full covariance matrix. The cell s.u.'s are taken into account individually in the estimation of s.u.'s in distances, angles and torsion angles; correlations between s.u.'s in cell parameters are only used

when they are defined by crystal symmetry. An approximate (isotropic) treatment of cell s.u.'s is used for estimating s.u.'s involving l.s. planes.

Refinement

Refinement of F2 against ALL reflections. The weighted R-factor wR and goodness of fit S are based on F2, conventional R-factors R are based on F, with F set to zero for negative F2. The threshold expression of $F2 > 2\sigma(F2)$ is used only for calculating R factors(gt) etc. and is not relevant to the choice of reflections for refinement. R-factors based on F2 are statistically about twice as large as those based on F, and R-factors based on ALL data will be even larger.

Figures

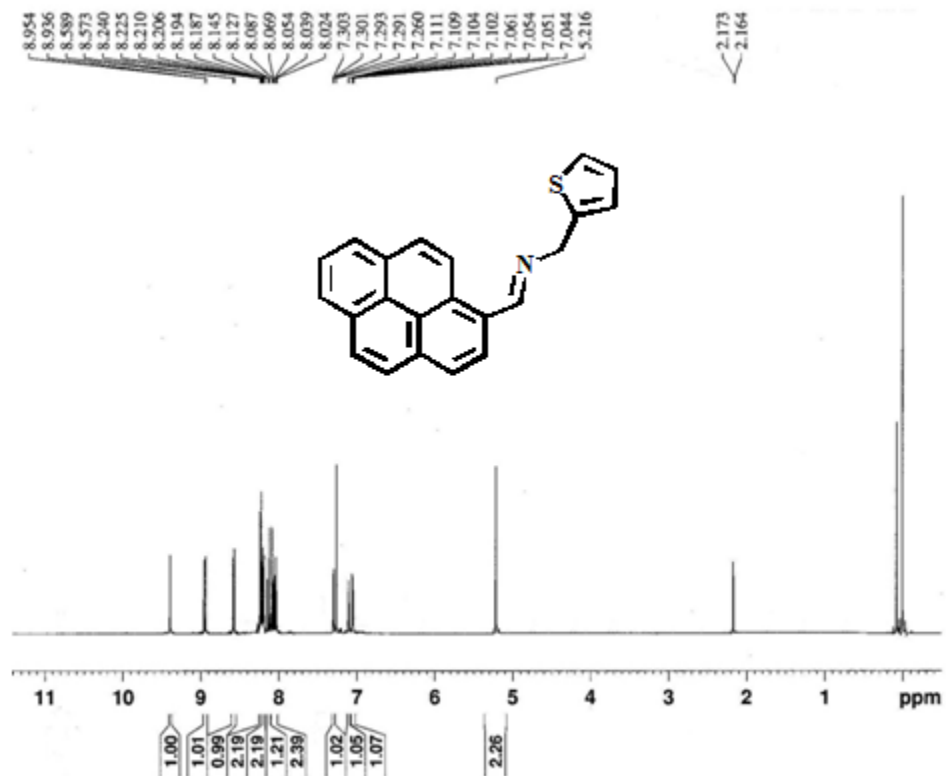


Figure S1. ^1H NMR spectrum of PTA in CDCl_3

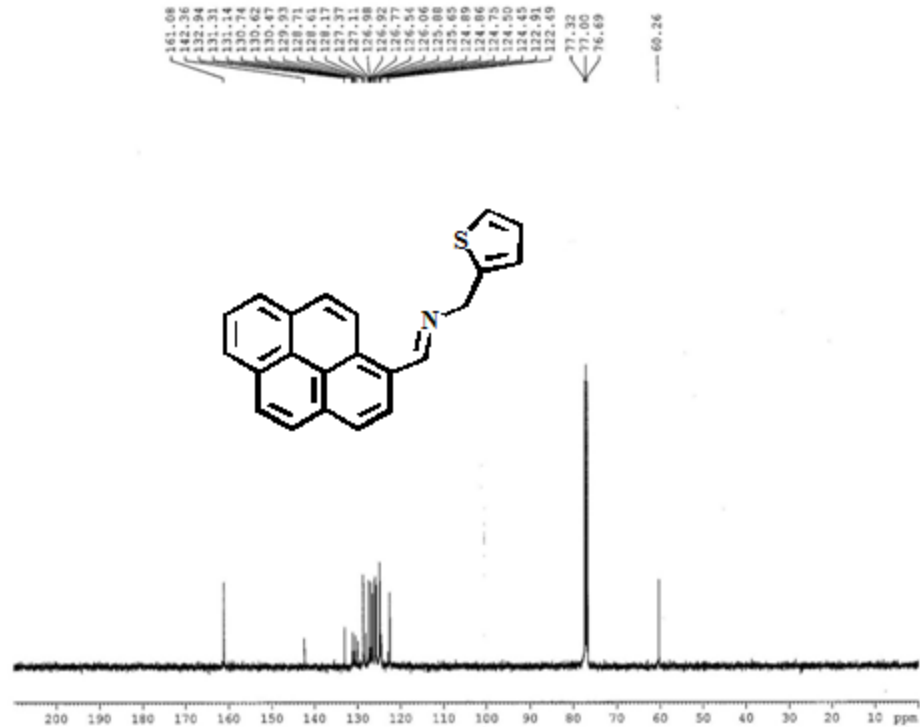


Figure S2. ^{13}C NMR spectrum of PTA in CDCl_3

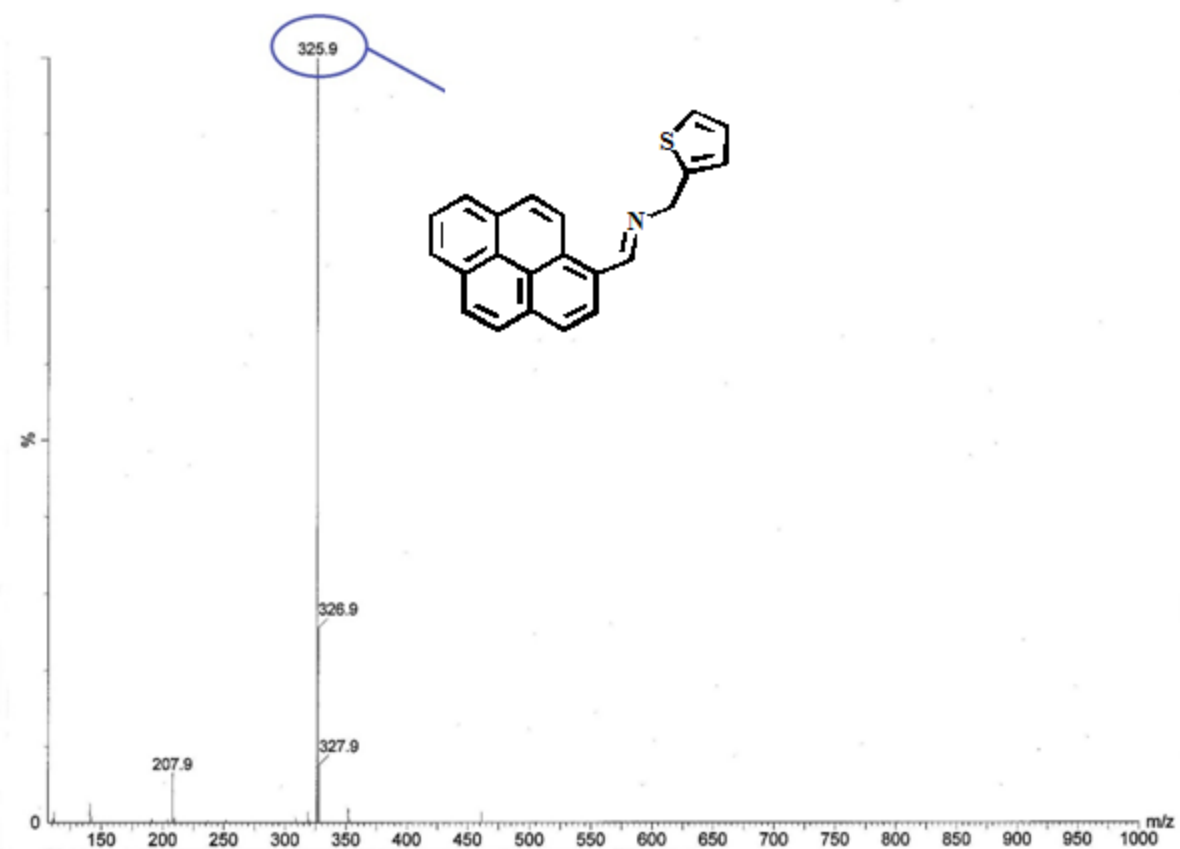


Figure S3. QTOF –MS ES⁺ spectrum of PTA

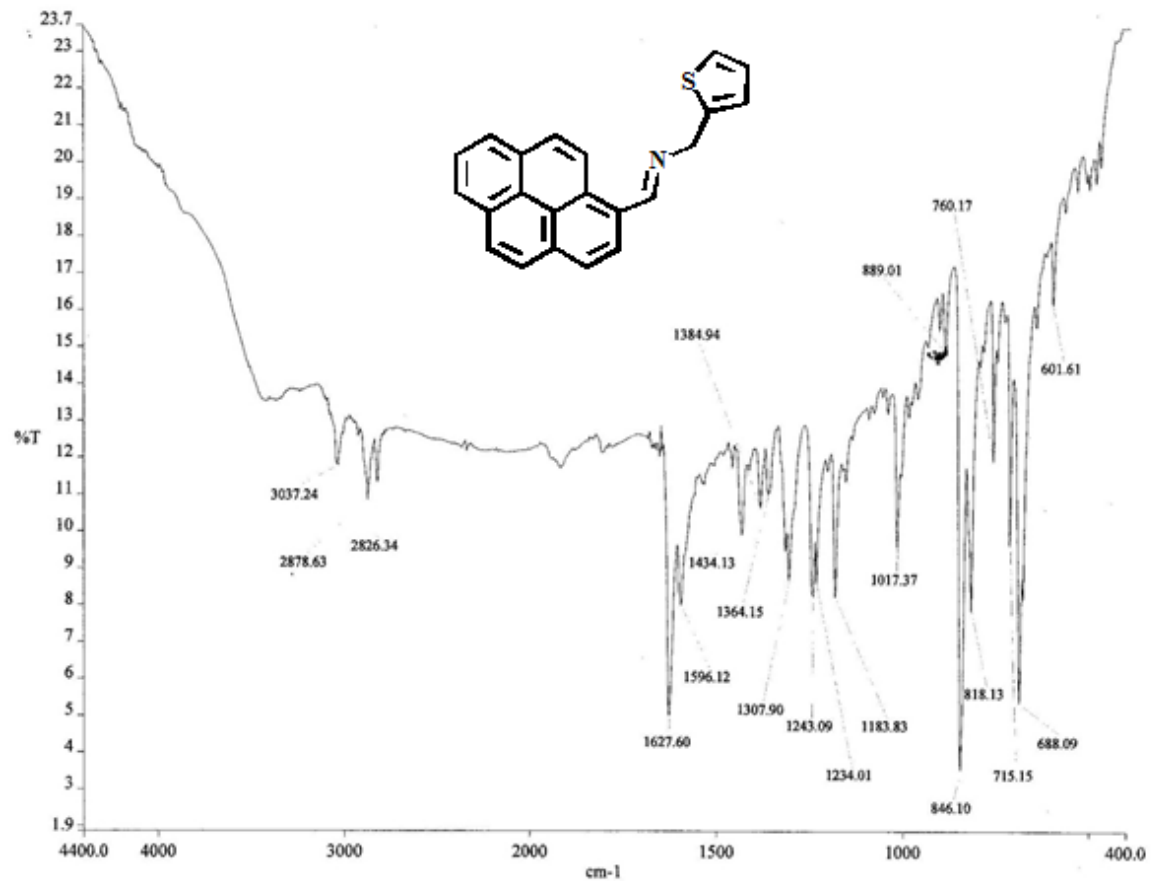


Figure S4. FTIR spectrum of PTA

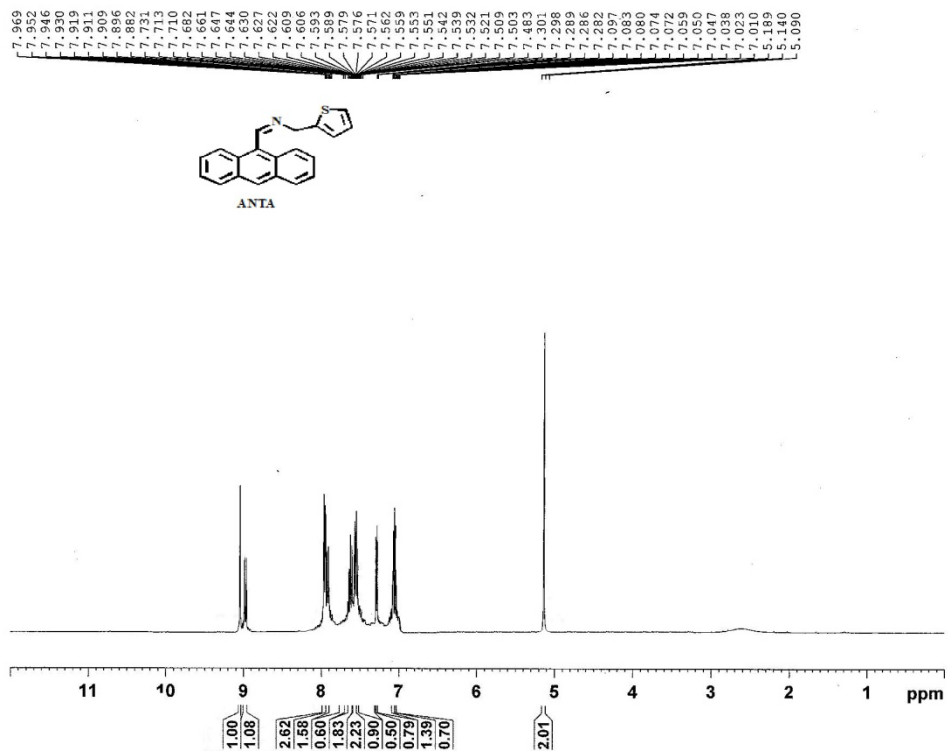


Figure S5. ¹H NMR spectrum of ANTA in CDCl_3

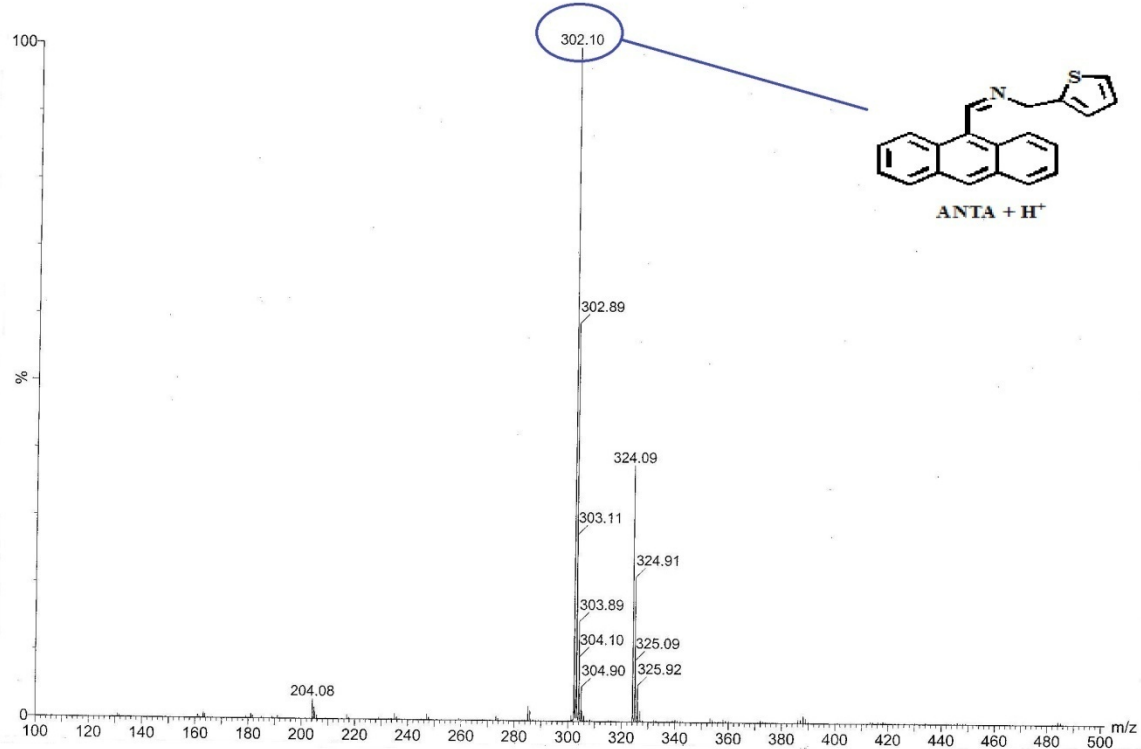


Figure S6. QTOF –MS ES^+ spectrum of ANTA

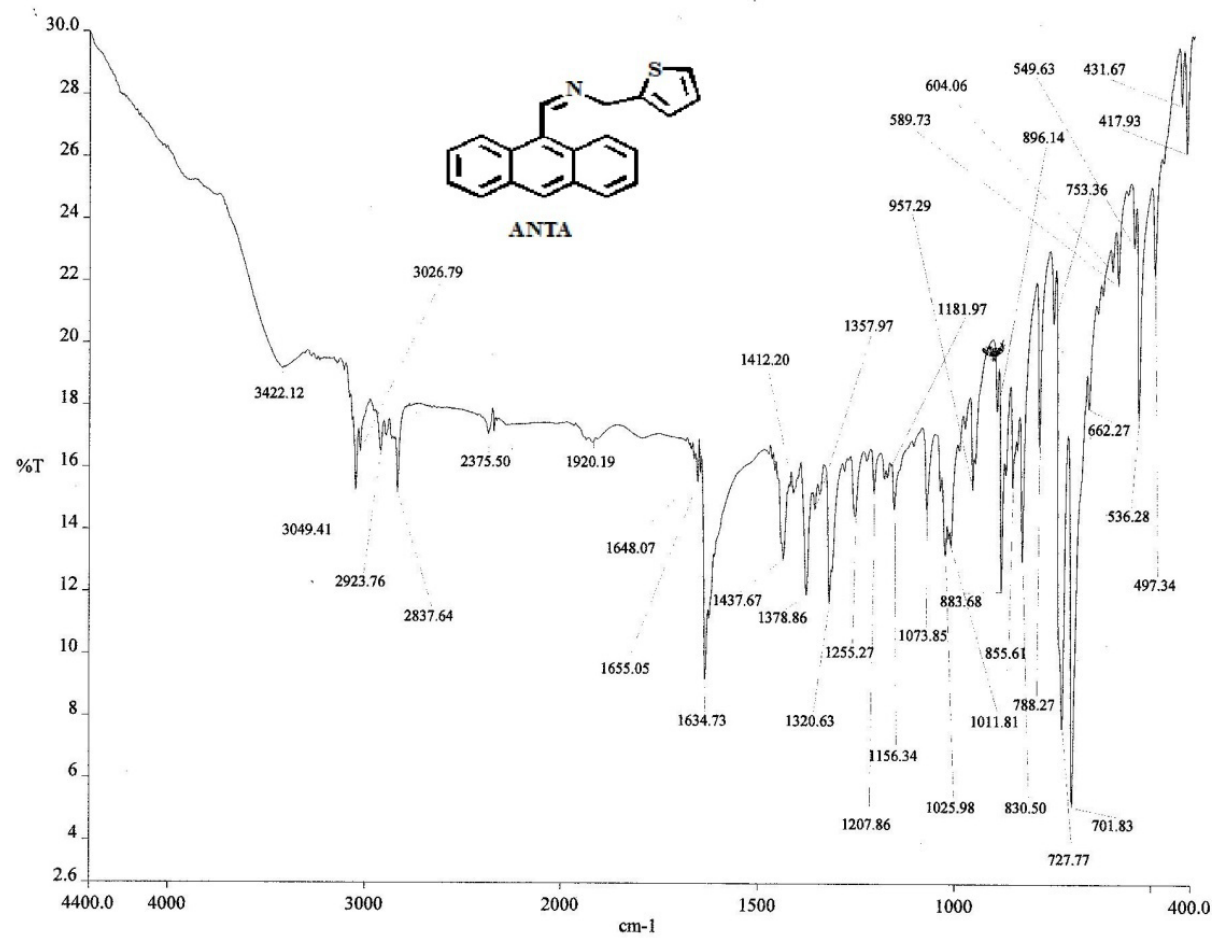


Figure S7. FTIR spectrum of ANTA

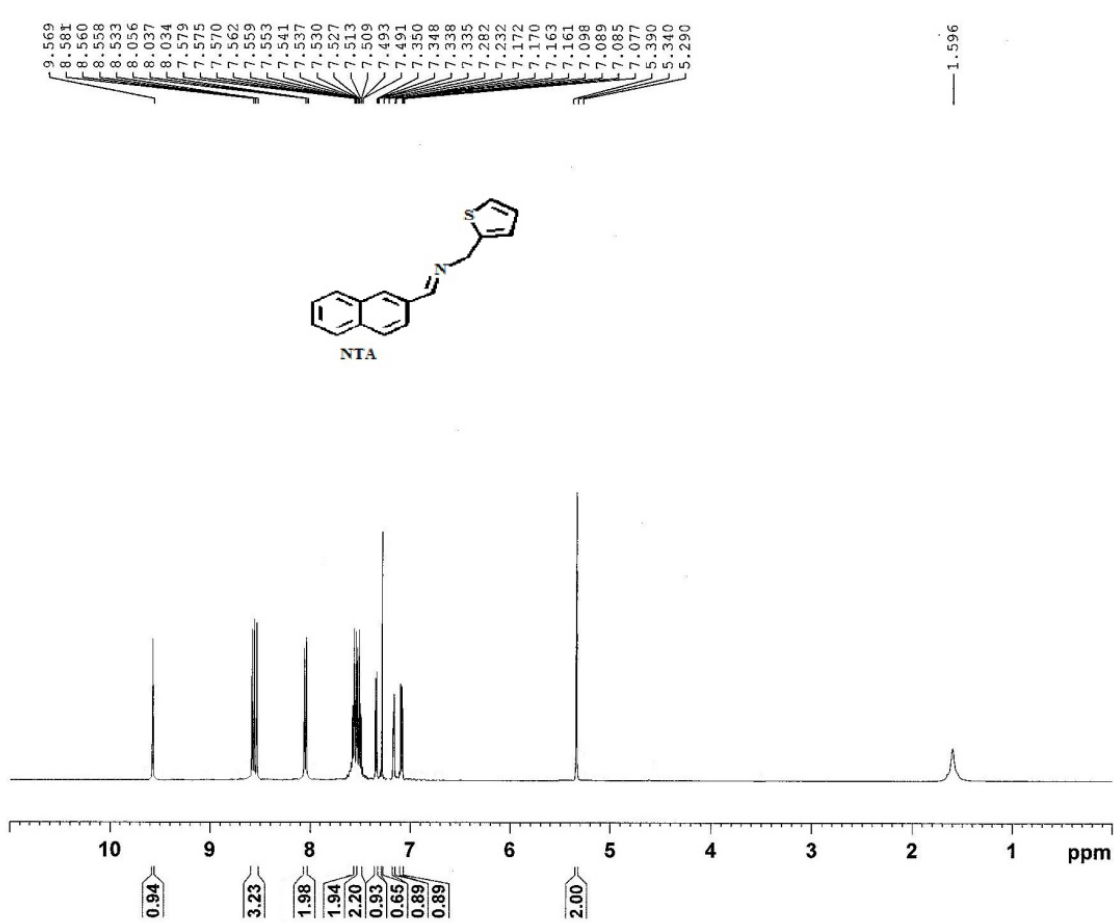


Figure S8. ^1H NMR spectrum of NTA in CDCl_3

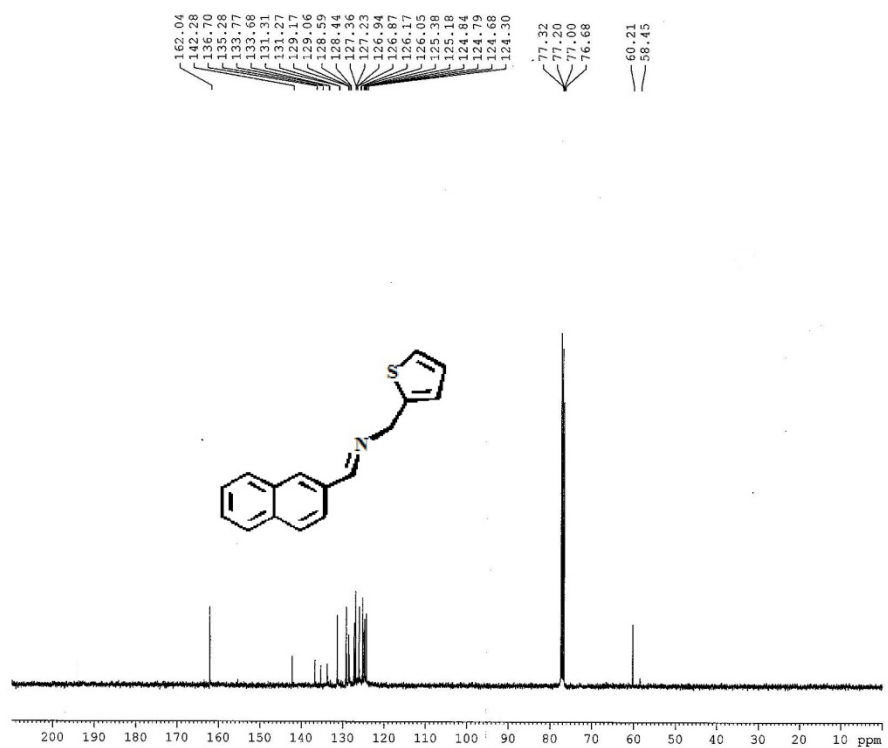


Figure S9. ^{13}C NMR spectrum of NTA in CDCl_3

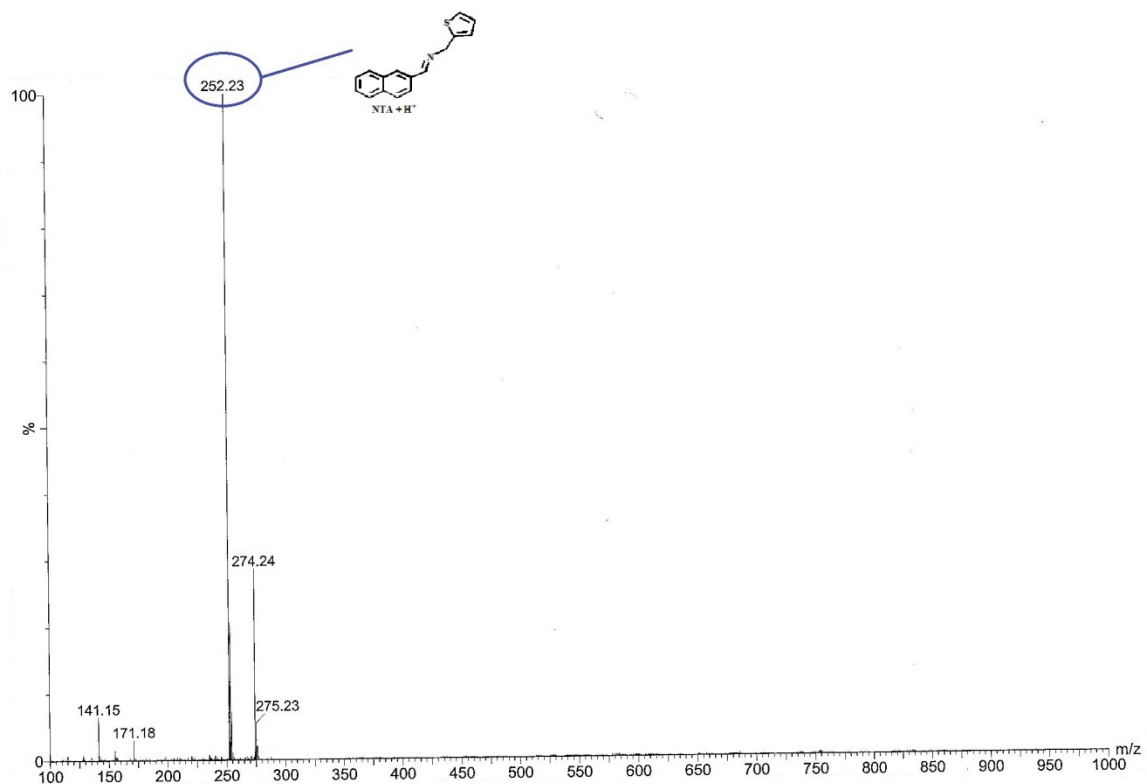


Figure S10. QTOF –MS ES⁺ spectrum of NTA

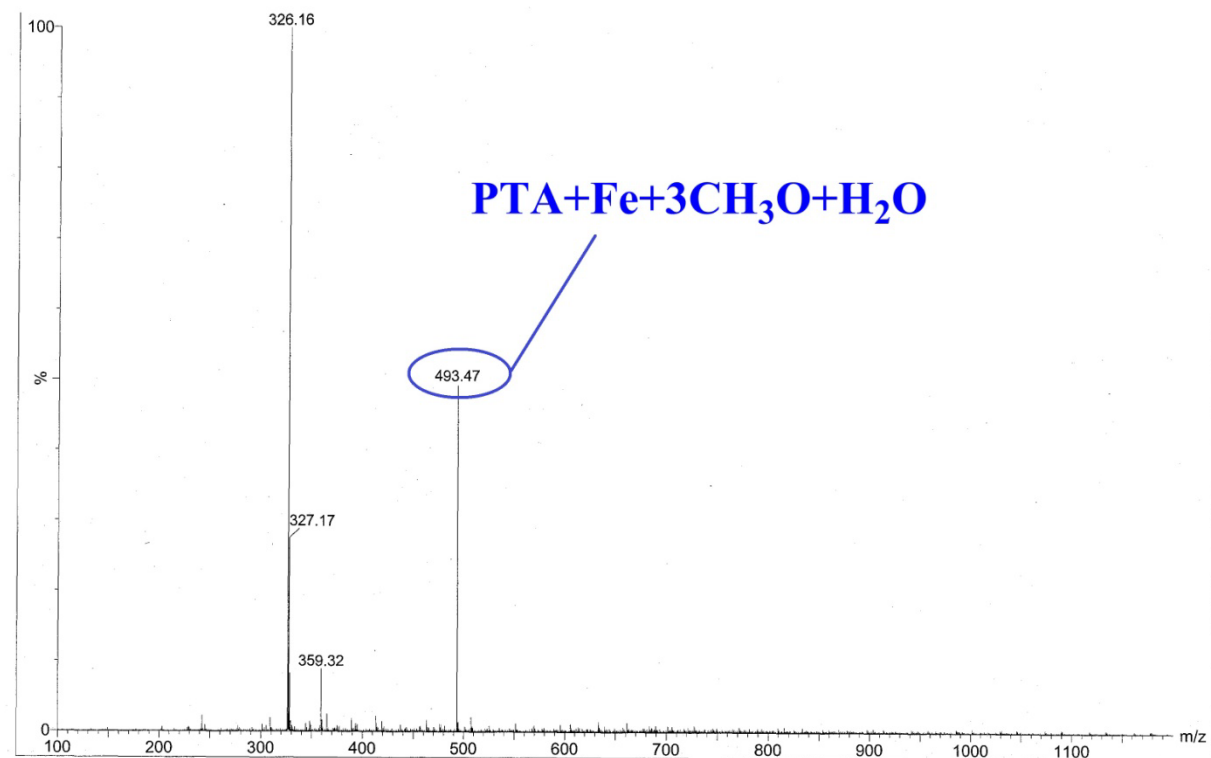


Figure S11. QTOF –MS ES⁺ spectrum of [PTA-Fe³⁺] adduct

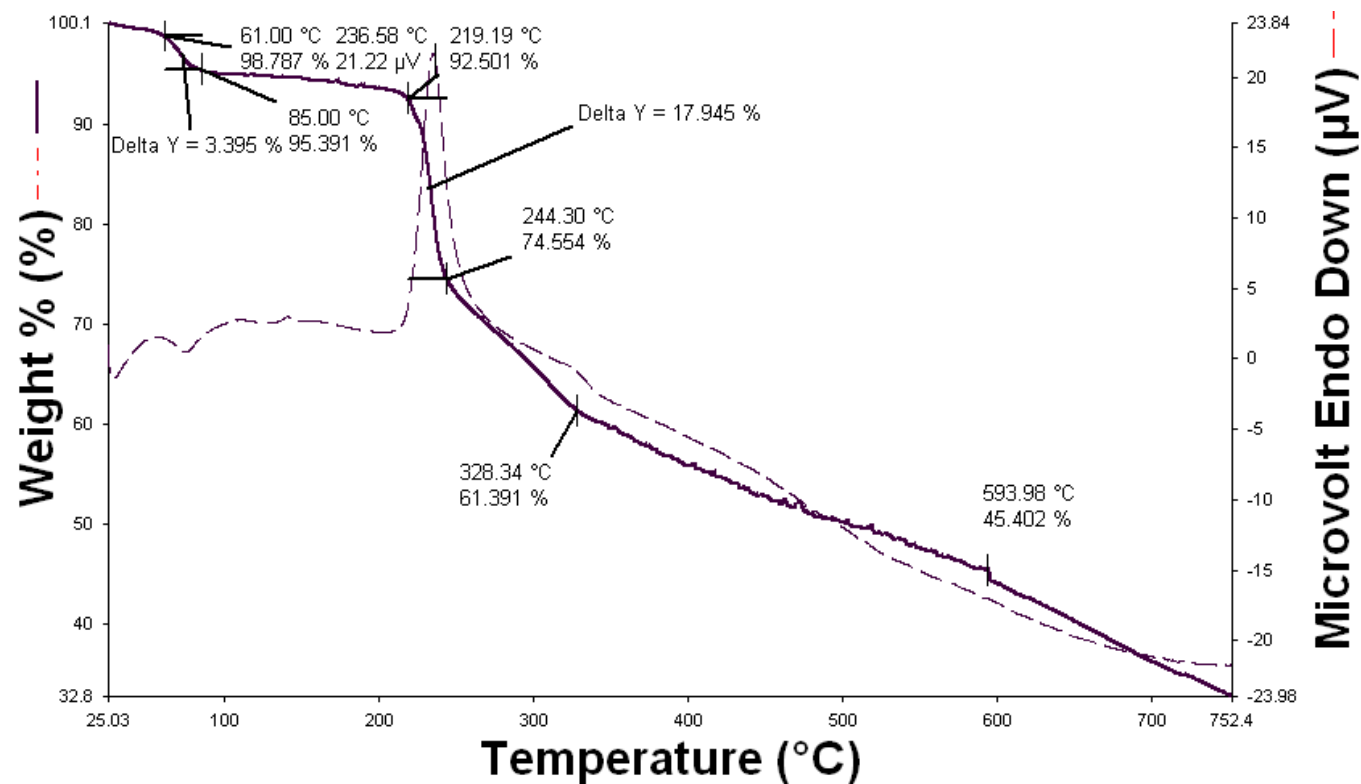


Figure S12. Thermogram of the $[\text{PTA}-\text{Fe}^{3+}]$ adduct

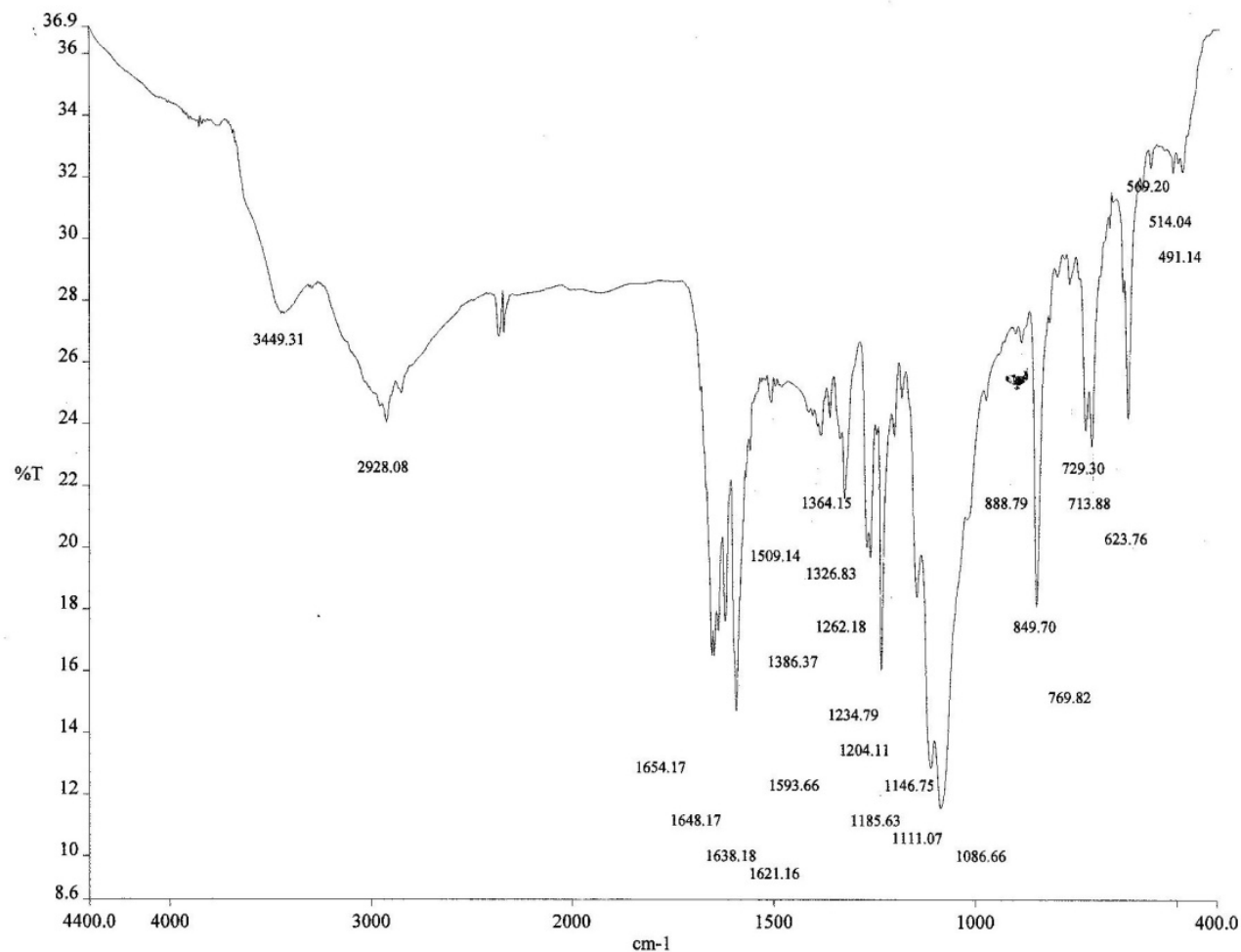


Figure S13. FTIR spectrum of the [PTA-Fe³⁺] adduct

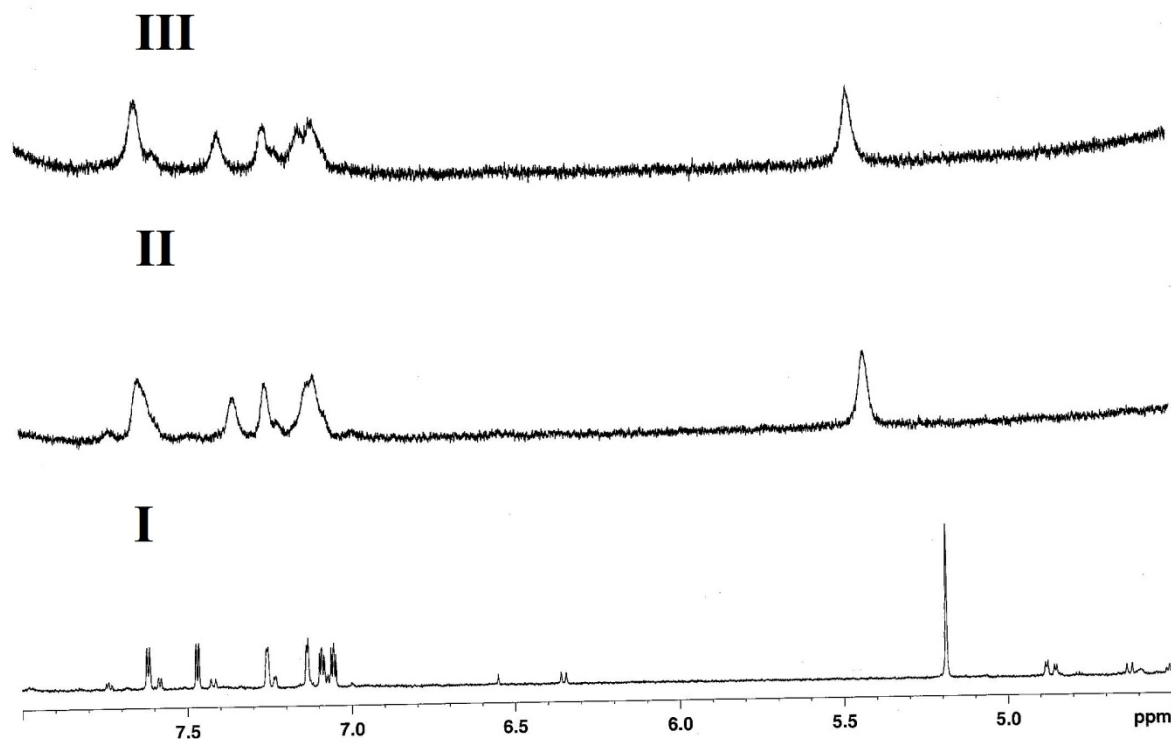


Figure S14. ¹H NMR spectra of **PTA** with Fe³⁺ in DMSO-d₆: (I) only **PTA**; (II) **PTA** with 1 equiv. of Fe³⁺; (III) **PTA** with 2.0 equiv. of Fe³⁺.

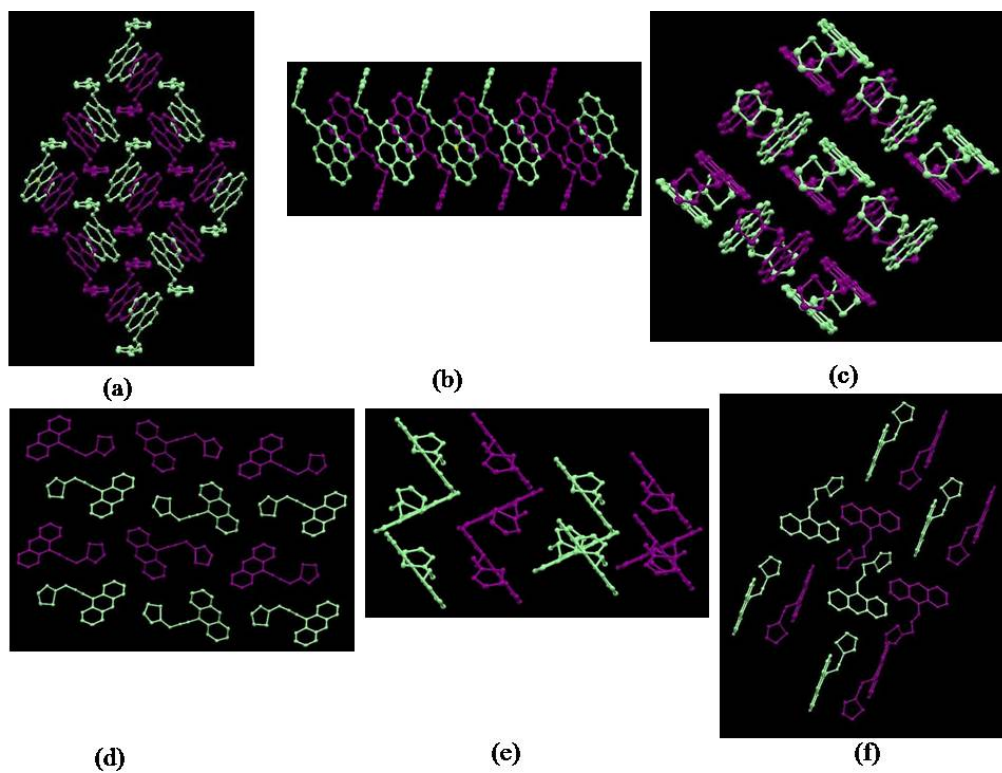


Figure S15. Crystal packing diagram of PTA (a), (b) and (c) and ANTA (d), (e) and (f) along three different axis a, b and c respectively.

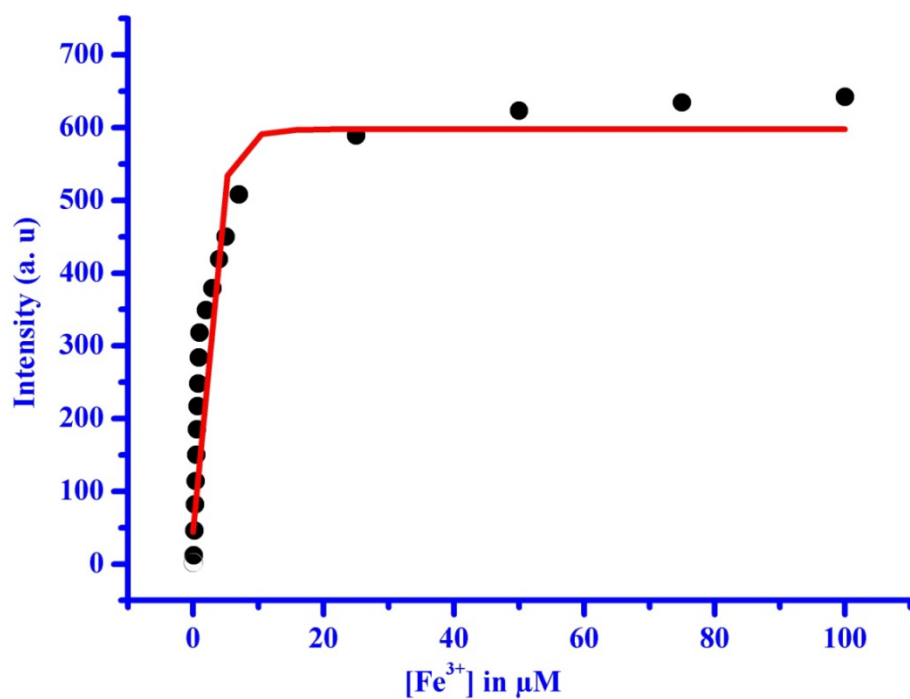


Figure S16. Plot of fluorescence intensity vs. externally added $[\text{Fe}^{3+}]$ (1–100 μM)

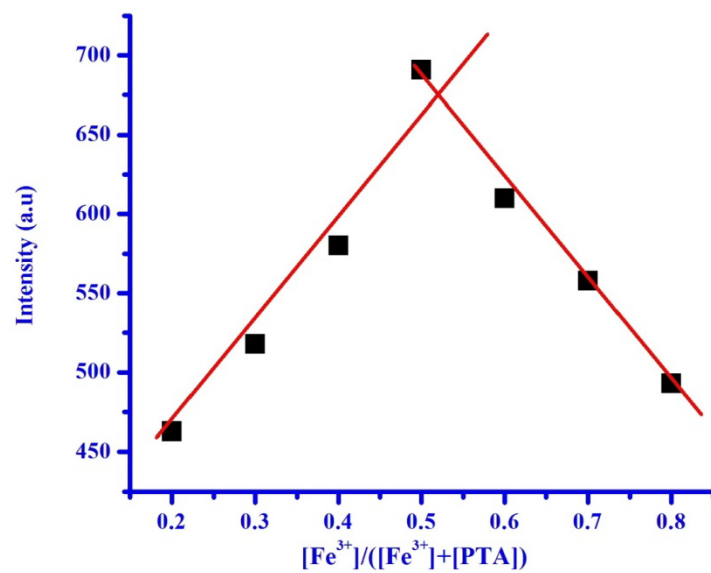


Figure S17. Job's plot for determination of stoichiometry of the [PTA- Fe^{3+}] system.

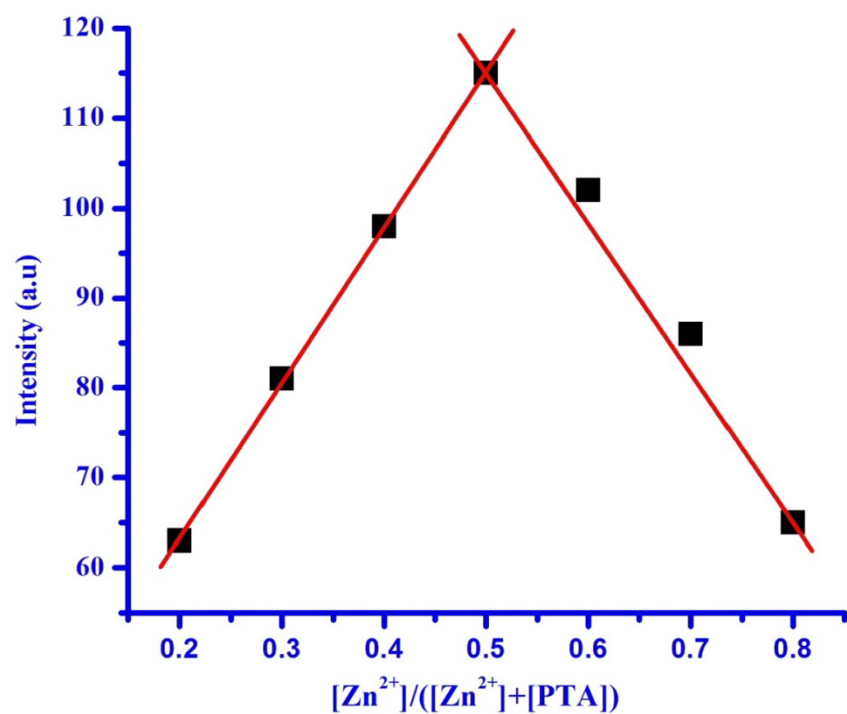


Figure S18. Job's plot for determination of stoichiometry of the [PTA-Zn²⁺] system

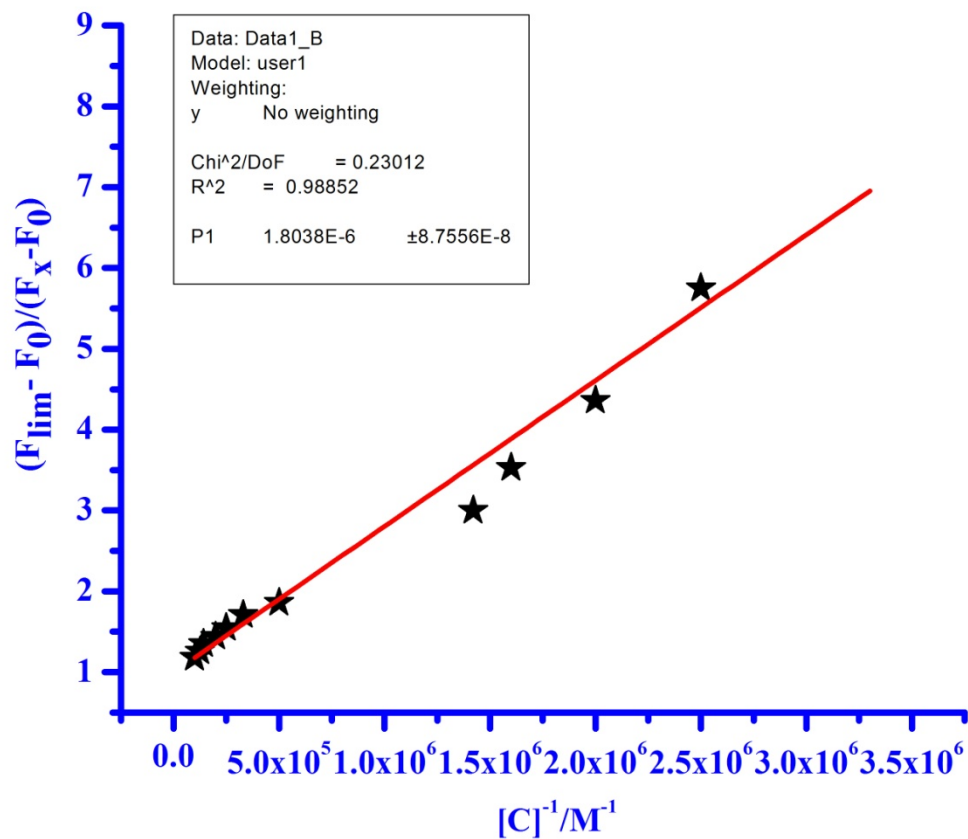


Figure S19. Determination of the binding constant of **PTA** with Fe^{3+} using $(F_{\text{max}} - F_0)/ (F_x - F_0) = 1 + (1/K) \times (1/[M]^n)$, where F_{max} , F_0 and F_x are fluorescence intensities of **PTA** in presence of Fe^{3+} at saturation, free **PTA** and at any intermediate Fe^{3+} concentration, respectively.

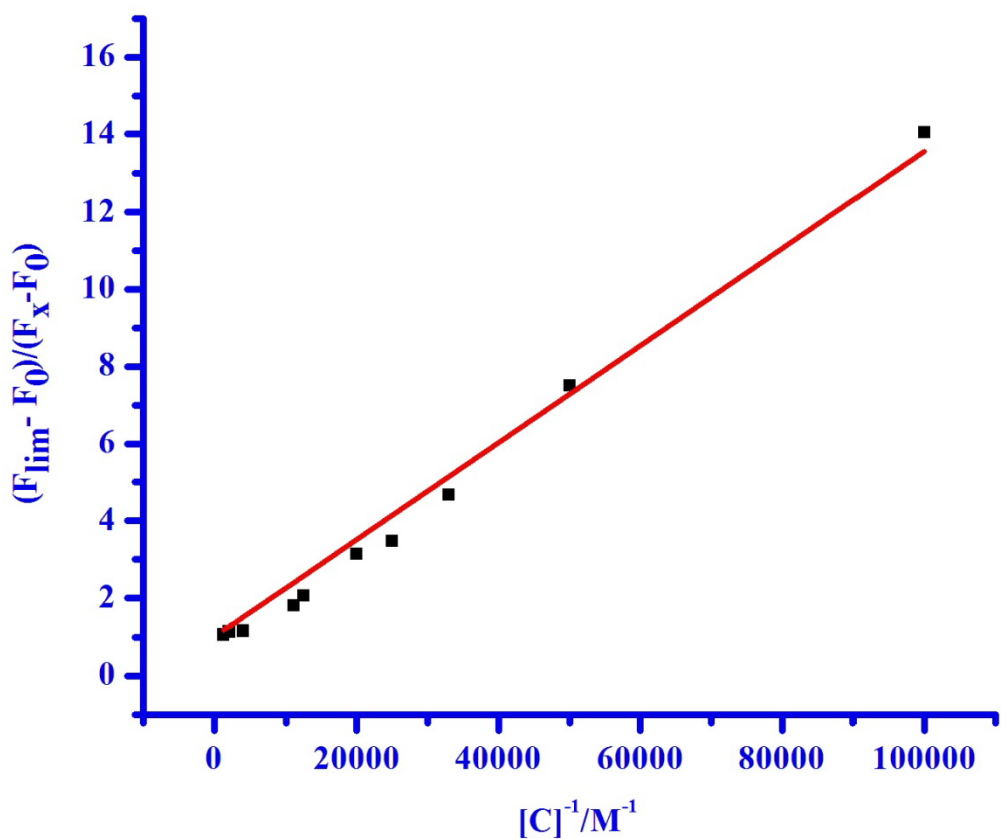


Figure S20. Determination of the binding constant of **PTA** with Zn^{2+} using $(F_{\text{max}} - F_0)/ (F_x - F_0) = 1 + (1/K) \times (1/[M]^n)$, where F_{max} , F_0 and F_x are fluorescence intensities of **PTA** in presence of Zn^{2+} at saturation, free **PTA** and at any intermediate Zn^{2+} concentration, respectively.

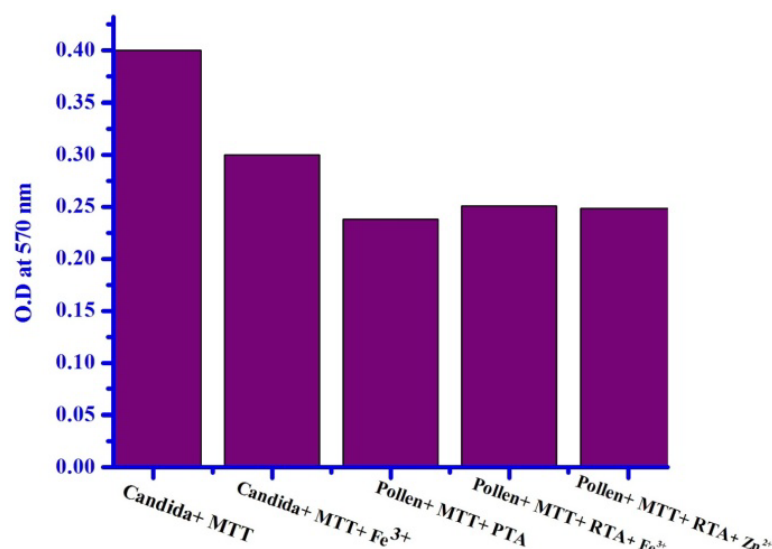


Figure S21. MTT assay studies of PTA.

References

1. E. Austin, M. Gouterman, *Bioinorg. Chem.*, 1978, **9**, 281.
2. W. H. Melhuish, *J. Phys. Chem.*, 1961, **65**, 229.
3. J. V. Houten, R. J. Watts, *J. Am. Chem. Soc.*, 1976, **98**, 4853.
4. G. L. Long, J. D. Winefordner, *Anal. Chem.*, 1983, **55**, 712A.